Liquid Crystals
Publication details, including instructions for authors and subscription information:
http://www.informaworld.com/smpp/title~content=t713926090

Periodic deformations induced by a magnetic field in planar twisted nematic layers

Dariusz Krzyzański; Grzegorz Derfel

Online publication date: 11 November 2010

LIQUID CRYSTALS, 2002, VOL. 29, NO. 7, 951–959

Taylor & Francis
Taylor & Francis Group

Periodic deformations induced by a magnetic field in planar twisted nematic layers

DARIUSZ KRZYŻAŃSKI* and GRZEGORZ DERFEL
Institute of Physics, Technical University of Łódź, ul. Wólczańska 219, 93-005 Łódź, Poland

(*Received 19 January 2002; accepted 1 March 2002*)

Magnetic field-induced spatially periodic deformations of planar nematic layers twisted by an angle Φ were investigated numerically. Chiral nematics with pitches compatible with the twist angle and non-chiral nematics twisted by $\Phi \leqslant \pi/2$ were considered. Two different modes of deformation, taking the form of stripes, were found: the so called Mode X, with periodicity parallel to the mid-plane director in the undisturbed structure, and Mode Y with periodicity perpendicular to the mid-plane director. The static director distributions were calculated for various magnetic field strengths, twist angles and elastic parameters. The influence of surface tilt was also investigated. Mode X appeared for sufficiently large Φ and was possible in nematics with typical elastic properties. Mode Y appeared provided that the k_{22}/k_{11} elastic constant ratio and the twist angle Φ were sufficiently small. Both modes arose from the undistorted state when the magnetic field exceeded a threshold value. The spatial period of the patterns increased with field strength. At high field, regions with almost homogeneous deformation arose in the two halves of each stripe. Their width and, simultaneously, the spatial period diverged to infinity at some critical field. This divergence corresponds to the transition to a homogeneously deformed state. Diagrams were constructed showing the ranges of parameters favouring the periodic distortions.

1. Introduction

The magnetic or electric field-induced deformations of the director distribution in liquid crystal layers can have a two-fold character. The most common deformations are the homogeneous deformations (HD) which have the same form and magnitude over the whole layer area subjected to the field. The successful applications of nematic liquid crystals are based on these deformations. Another possibility involves the spatially periodic distortions (PD) observed for instance as a pattern of parallel stripes [1, 2]. This paper is devoted to numerical studies of the periodic distortions appearing in planar layers of twisted chiral and non-chiral nematics subjected to a magnetic field. The phenomena occurring in an electric field are qualitatively the same, but they involve some additional effects which make their analysis somewhat more complex.

Let us consider a planar, rigidly aligned twisted nematic liquid crystal layer of thickness d placed between two plates parallel to the (x, y) plane in a Cartesian co-ordinate system. Initially, in the undistorted state of the layer (US), the director is parallel to the boundary planes and uniformly twisted by an angle Φ. The magnetic field applied parallel to the z axis deforms the director distribution $\mathbf{n}(\mathbf{r})$ due to the positive diamagnetic anisotropy $\Delta\chi$. The director orientation can be described by two angles: the tilt angle θ, between the (x, y) plane and $\mathbf{n}$, and the azimuthal angle φ, between the x axis and the projection of $\mathbf{n}$ on the (x, y) plane.

The homogeneous deformation occurs above the threshold magnetic field given by [3]:

$$H_{\mathrm{TN}} = (\pi/d)\left(\frac{k_{11}}{\Delta\chi}\right)^{1/2}\left[1 + \left(\frac{\Phi}{\pi}\right)^2 (k_{\mathrm{b}} - 2k_{\mathrm{t}}) + 4k_{\mathrm{t}}\frac{d\Phi}{p\,\pi}\right]^{1/2} \quad (1)$$

where p is the intrinsic pitch, and k_{t} and k_{b} denote the elastic constants ratios: $k_{\mathrm{t}} = k_{22}/k_{11}$ and $k_{\mathrm{b}} = k_{33}/k_{11}$. In this case, the angles θ and φ depend only on the z co-ordinate and are given by the even function $\theta(z)$ and the odd function $\varphi(z)$.

In the case of periodic deformations, both angles depend on a pair of co-ordinates: z and x or z and y, according to the two types of pattern called Mode X and Mode Y, respectively [4, 5]. The stripes of Mode X are perpendicular to the mid-plane director in the undistorted structure. They were observed by Chigrinov *et al.* in a nematic mixture containing chiral dopant [1]. The stripes were induced by the electric field in wedge-shaped layers with planar boundary conditions and with crossed or parallel easy axes. They are also known as an unwanted

*Author for correspondence; e-mail: dkryzan@ck-sg.p.lodz.pl

Liquid Crystals ISSN 0267-8292 print/ISSN 1366-5855 online © 2002 Taylor & Francis Ltd
http://www.tandf.co.uk/journals
DOI: 10.1080/02678290210145157

effect appearing in super-twisted nematic display cells [6]. Mode Y, with stripes parallel to the mid-plane director, can be interpreted as a twisted version of the periodic splay–twist (PST) deformation, observed first by Lonberg and Meyer [2] in an untwisted layer of polymer nematic PBG. Periodic deformations in twisted layers were also analysed theoretically by the use of linearized equations [4, 5, 7] and by the perturbation method [8–11].

Kini [4, 5] investigated a layer of non-chiral nematic twisted by $\Phi < \pi/2$ subjected to a magnetic field. The threshold for the transition US $\rightarrow$ PD (lower than H_{TN}) and the wave number of PD at the threshold were found for both modes. The wave number decayed to 0 for critical Φ values which limited the range of twist angles for Mode X from below and for Mode Y from above. The director deformation in Mode X was described by even $\theta(z)$ and $\varphi'(z)$ functions (where $\varphi'(z)$ measures the difference between deformed and undeformed $\varphi(z)$ values) which was not in conformity with the HD state. Even $\theta(z)$ and odd $\varphi'(z)$ functions were used for Mode Y. Mode Y was found to arise for small twist angles, whereas Mode X arose for sufficiently large twist angles. Very low values of k_t were necessary for Mode Y. Mode X was favoured by high k_b and low k_t. For some ranges of elastic constants and twist angles the possibility of coexistence of both modes was found.

The analysis made by Schiller [8–11] confirmed the main results of Kini it concerns the stripes arising under the action of an electric field in planar cholesteric layers. The US $\rightarrow$ PD transition was recognised as continuous, and the PD $\rightarrow$ HD transition as discontinuous. Phase diagrams showing the ranges of existence of the stripes in the (voltage, k_t) plane were presented. They possessed a characteristic wedge-like shape. Mode X was found to exist for k_t lower than some critical value increasing with k_b.

Schiller [8] as well as Tsoy *et al.* [7] also analysed the influence of surface tilt on the occurrence of the stripes. It was shown that occurrence of the PD can be strongly limited by tilt angles of the order of several degrees.

The aim of our work was to investigate numerically the structure of the stripes over the whole range of the magnetic field inducing them, and to determine the conditions for their appearance. The roles of the elastic properties of the nematic liquid crystal, of the magnetic field strength and of the twist angle for the occurrence of PD from US, as well as for the occurrence of the PD $\rightarrow$ HD transition, have been analysed. Chiral nematics with pitch values compatible with the twist angle, as well as non-chiral nematics were considered. The influence of the surface tilt has also been demonstrated.

In § 2, the details of the system under investigation are given and the method of computation is sketched. The results are presented in § 3, and § 4 is devoted to a short discussion.

2. Method

The calculations were performed for an infinite layer of nematic or chiral nematic of thickness d twisted by an angle Φ. Strong planar boundary anchoring was assumed. The liquid crystal was confined between two plates parallel to the (x, y) plane and positioned at $z = \pm d/2$. The undistorted director distribution was given by $\theta_0(z) = 0$ and $\varphi_0(z) = \Phi z/d$. The initial mid-plane director was parallel to the x axis. The external magnetic field was directed along the z axis. The director field deformations were described by means of two angles: θ and $\varphi' = \varphi - \varphi_0$. The angle φ' measured the azimuthal deviation of $\mathbf{n}$ from its initial orientation. The spatial periodicity of the deformations was characterized by the wave vectors $\mathbf{q} \parallel x$ and $\mathbf{q} \parallel y$ for Modes X and Y, respectively, or by the spatial period $\lambda = 2\pi/q$, where $q = |\mathbf{q}|$. The pitch p of the chiral nematic was compatible with the twist angle, $p = 2\pi d/\Phi$. The calculations were performed for Φ ranging from 0 to π. For $\Phi \leqslant \pi/2$, the twisted structure of the non-chiral nematic was also taken into account.

In most cases, the typical values $k_t = 0.6$ and $k_b = 1.5$ were adopted. Nevertheless, several small k_t ratios from the range 0.1–0.3 were also used. The role of k_b varying from 0.8 to 2.0 was investigated. The deviation from ideal planar anchoring was also considered in order to exemplify the changes in the Mode X structure. The surface tilt angles were varied between 0 and 0.1 rad.

The dimensionless quantities: $\xi = x/\lambda$, $\eta = y/\lambda$, $\zeta = z/d$, $h = H/H_{TN}$ and $Q = qd$ were used during the calculations. A single stripe of width λ was considered. Periodic boundary conditions along the $\mathbf{q}$ direction were imposed. The director distribution over the cross-section of the stripe, described by the functions $\theta(\xi, \zeta)$ and $\varphi(\xi, \zeta)$ (or by $\theta(\eta, \zeta)$ and $\varphi(\eta, \zeta)$), was approximated by discrete angles θ_{ij} and φ_{ij} defined in the sites of the regular lattice. The free energy per unit area of the layer was calculated by means of these, and minimized in the course of an iteration process involving the values of θ_{ij}, φ_{ij} and λ/d which were sequentially changed by small intervals. New values of the variables were accepted if they lowered the energy. This procedure was repeated until no further reduction of the total free energy could be achieved. Then the interval was decreased and the process was repeated. As a result, a state with minimum energy was obtained. A more detailed description can be found in our earlier papers [12, 13].

3. Results

In agreement with earlier theoretical predictions [4, 5, 7, 9], two types of periodic deformation with wave vectors $\mathbf{q} \| x$ and $\mathbf{q} \| y$, referred to as Mode X and Mode Y, were found. The director distributions were different in these modes. For the sake of clarity, the results will be presented separately for each mode.

3.1. *Mode X*

The wave vector of Mode X is parallel to the mid-plane director orientation in the undistorted layer $\mathbf{q} \| \mathbf{n}_0(\zeta=0)$. For small magnetic fields strengths, i.e. close to H_P, when the deformations are weak, the angles describing the director orientation are nearly sinusoidal functions of ξ and ζ with small amplitudes θ_m and φ'_m. The functions $\theta(\xi, \zeta)$ and $\varphi'(\xi, \zeta)$ are both even with respect to ζ, as was assumed in [4, 5]. In high fields, the distortion of the director distribution deviates from a sinusoidal form and the dependences $\theta(\zeta)$ and $\varphi'(\zeta)$ lose their symmetry. Large regions with almost homogeneous deformations of opposite sign appear within the two halves of the stripes, separated by narrow strongly deformed regions. The angles θ and φ' describing the director distribution in these homogeneous regions depend practically only on ζ. The symmetry properties of the corresponding $\theta(\zeta)$ and $\varphi'(\zeta)$ functions coincide with the symmetry of the homogeneously deformed layer, i.e. $\theta(\zeta)$ is even whereas $\varphi'(\zeta)$ is odd. A typical structure of a well developed stripe is presented as its cross-section in figure 1, where the cylinders symbolize the directors. The distortion of the director field in the same well developed stripe is determined quantitatively by the plots of the functions $\theta(\xi, \zeta)$ and $\varphi'(\xi, \zeta)$ shown in figure 2. Two halves with opposite signs of the angle θ can be distinguished within the stripe.

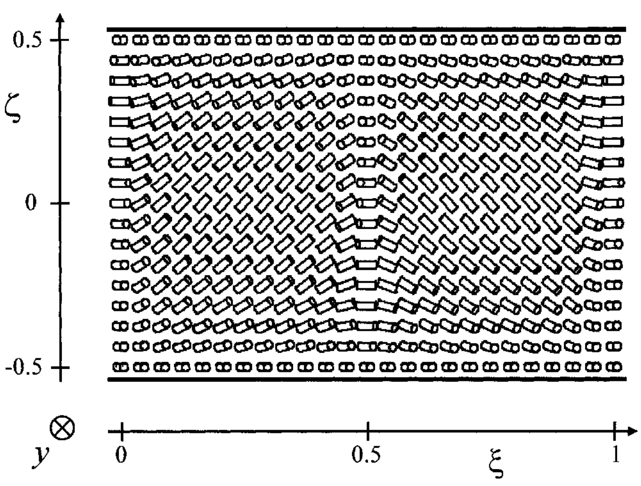

Figure 1. Example of the director distribution for a single stripe of Mode X: $\Phi = 2.4$ rad, $k_t = 0.6$, $k_b = 1.5$, $h = 1.065$, $\lambda = 6.83d$.

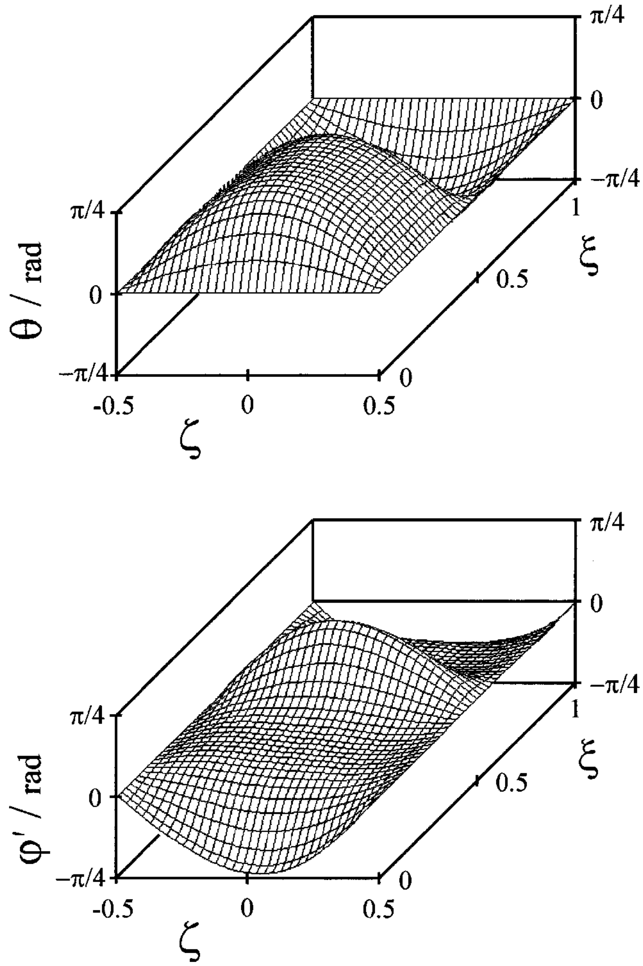

Figure 2. The angles θ and φ' for the typical well developed single stripe (see figure 1) of Mode X: $\Phi = 2.4$ rad, $k_t = 0.6$, $k_b = 1.5$, $h = 1.065$, $\lambda = 6.83d$.

The stripes arise continuously from the undistorted state at a critical field $h_P = H_P/H_{TN} < 1$ and have finite initial width. The magnetic field influences the spatial period as illustrated in figure 3 by the plots $Q(h)$, calculated for chosen Φ and material parameters. Typically, λ increases with magnetic field strength and tends rapidly to infinity at a reduced critical field h_D. (A slight decrease in the spatial period with increasing h is sometimes observed in the vicinity of h_P for large twist angles or low k_t.) The nearly homogeneous regions spread over the whole layer above h_D. As a result, the PD state transforms into the homogeneously deformed state.

The range of magnetic field strengths which induce the stripes is given by the difference $\Delta h = h_D - h_P$. It depends on the twist angle Φ and on the material parameters k_t and k_b. The dependence of Δh on the twist angle is shown in figure 4 in the plane (Φ, h) for chosen sets of material parameters. For given elastic constants ratios, Δh narrows with decreasing Φ and decays to

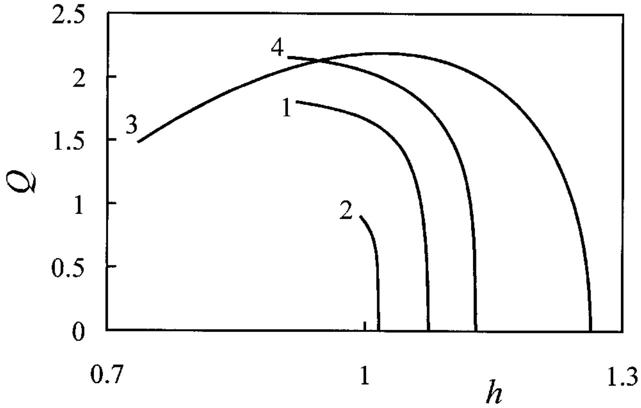

Figure 3. The dimensionless wave number Q of Mode X as a function of the reduced magnetic field strength h. Curve 1: $\Phi = 2.4$ rad, $k_t = 0.6$, $k_b = 1.5$; curve 2: $\Phi = 1.6$ rad, $k_t = 0.6$, $k_b = 1.5$; curve 3: $\Phi = 2.4$ rad, $k_t = 0.1$, $k_b = 1.5$; curve 4: $\Phi = 2.4$ rad, $k_t = 0.6$ $k_b = 0.8$.

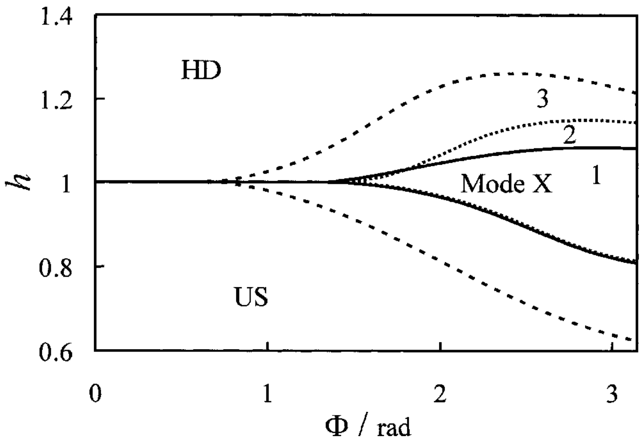

Figure 4. The ranges of existence of Mode X in the (Φ, h) plane. Region 1: $k_t = 0.6$, $k_b = 1.5$; region 2: $k_t = 0.6$, $k_b = 0.8$; region 3: $k_t = 0.1$, $k_b = 1.5$. The lower boundary of the regions 1 and 2 almost overlap.

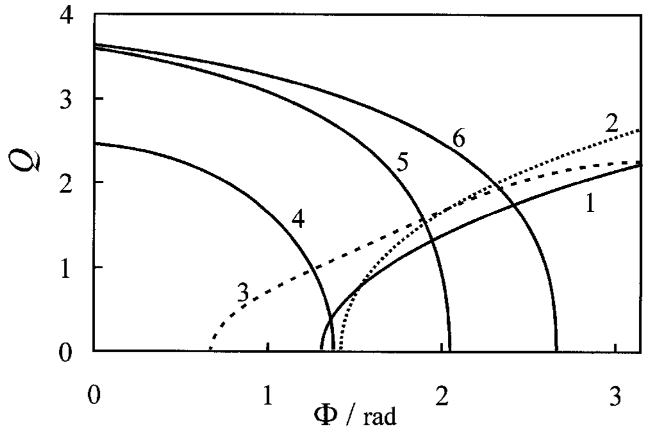

Figure 5. The dimensionless wave number Q at $h = 1$ as a function of the twist angle Φ for Mode X (curves $1 \rightarrow 3$) and Mode Y (curves $4 \rightarrow 6$). 1: $k_t = 0.6$, $k_b = 1.5$; 2: $k_t = 0.6$, $k_b = 0.8$; 3: $k_t = 0.1$, $k_b = 1.5$; 4: $k_t = 0.2$, $k_b = 1.5$; 5: $k_t = 0.1$, $k_b = 1.5$; 6: $k_t = 0.1$, $k_b = 0.8$.

0 ($h_D = h_P = 1$) at a critical minimum twist angle Φ_X. For $\Phi < \Phi_X$, only the homogeneously deformed and undistorted states are possible. It is evident, that the range of Φ which favours the X stripes is the widest for $h = 1$. The spatial period determined at constant field $h = 1$ diverges to infinity when Φ tends to Φ_X (as shown in figure 5), whereas the amplitudes θ_m and φ'_m decay to zero.

From figures 4 and 5 one can find the influence of k_t and k_b on the magnetic field range Δh as well as on the critical twist angle Φ_X. The significant increase of Φ_X and decrease of Δh with k_t are observed. The influence of the k_b ratio is weaker. Whereas h_D decreases with k_b, variation of h_P is not considerable. The lower boundaries of regions 1 and 2 in figure 4 (corresponding to $k_b = 1.5$ and $k_b = 0.8$, respectively) practically coincide, but Φ_X is slightly smaller for the bigger k_b ratio.

For constant Φ and k_b, one can construct a diagram showing the dependence of Δh on k_t in the (k_t, h) plane. It also possesses a wedge-like shape similar to that presented in figure 4 and therefore it is not presented here. The range of k_t favouring the stripes is the biggest for $h = 1$. For fixed Φ and k_b, there exists a critical value of k_t above which the stripes are forbidden. The spatial period diverges to infinity when k_t tends to this critical value. The critical k_t increases with Φ as shown in figure 6 for constant $k_b = 1.5$ (curve 1). It is evident that Mode X should be observable for any chiral nematic liquid crystal with a typical value of k_t if only Φ has a sufficiently high value.

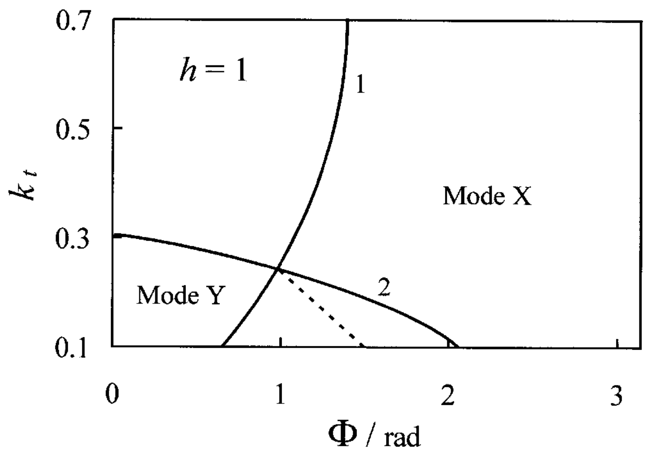

Figure 6. The ranges of k_t and Φ favouring Mode X (below the curve 1) and Mode Y (below the curve 2); $h = 1$; $k_b = 1.5$. The dashed line is the approximate boundary between the two modes corresponding to their having equal energies.

3.2 *Mode Y*

The stripes of Mode Y are perpendicular to those of the Mode X patterns. Their wave vector **q** is normal to the mid-plane director orientation in the undistorted layer. A typical director distribution within the cross-section of a well developed stripe is illustrated in figure 7. Two halves of the stripe with opposite senses of director distortion can be distinguished. The structure of this stripe determined by the functions $\theta(\eta,\zeta)$ and $\varphi'(\eta,\zeta)$ is shown in figure 8. The function $\theta(\eta,\zeta)$ is even and the function $\varphi'(\eta,\zeta)$ is odd with respect to ζ, according to [4, 5]. This structure can be recognized as a twisted version of the periodic splay-twist patterns (PST) [4, 12] which were observed for $\Phi = 0$ [2]. The characteristic features of Mode Y are analogous to those of the PST. In particular, the values of k_t favouring the stripes must be sufficiently low. The limiting value is lower than $k_t = 0.303$ which agrees with that for $\Phi = 0$ [14, 15], and decreases with Φ. This is shown in figure 9 by the plots of $Q(k_t)$ functions calculated for $h = 1$, $k_b = 1.5$ and chosen values of Φ. The spatial period tends to infinity when k_t approaches the corresponding limiting value.

Small distortions are described by the angles nearly sinusoidally dependent on η and ζ. In higher fields, large regions with almost homogeneous deformations of opposite sign develop within two halves of the stripes. The symmetry properties of the angles θ and φ' remain unchanged and they correspond to the homogeneously deformed layers.

As before, stripes arise continuously from the undistorted state at a critical field $h_P < 1$. The plots $Q(h)$ shown in figure 10 illustrate the dependence of the stripe width on the magnetic field strength. The divergence of the spatial period λ at a critical field h_D leads to transition to the HD state. A slight decrease in spatial period with increasing h is also observed in the vicinity of h_P.

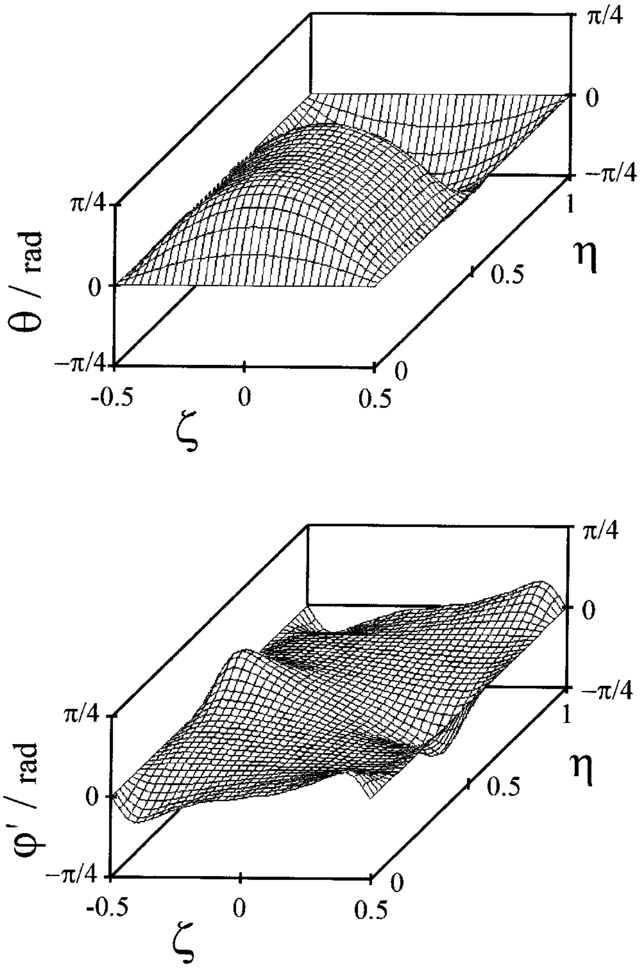

Figure 8. The angles θ and φ' for a typical well developed single stripe of Mode Y: $\Phi = 0.6$ rad, $k_t = 0.1$, $k_b = 1.5$, $h = 1.25$, $\lambda = 3.66d$.

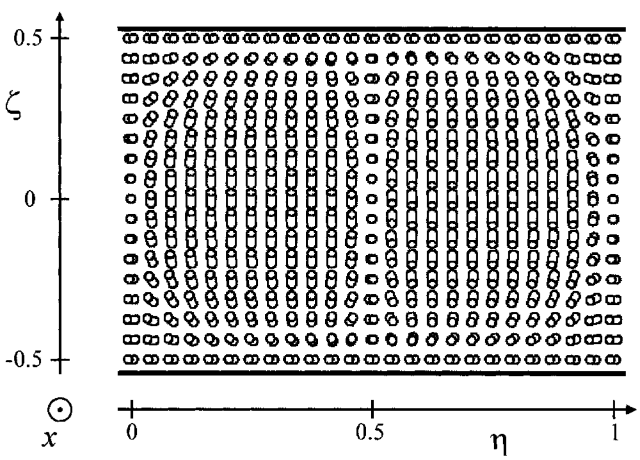

Figure 7. Typical director distribution for a single stripe of Mode Y: $\Phi = 0.6$ rad, $k_t = 0.1$, $k_b = 1.5$, $h = 1.25$, $\lambda = 3.66d$.

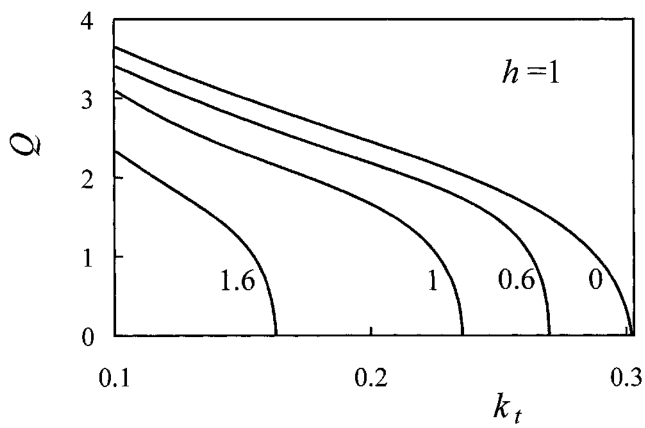

Figure 9. The dimensionless wave number Q of Mode Y as a function of the elastic constant ratio k_t. The twist angle values are indicated on each curve; $k_b = 1.5$; $h = 1$.

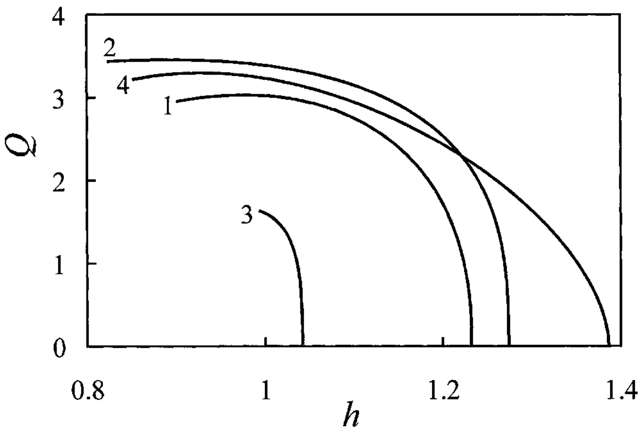

Figure 10. The dimensionless wave number Q of Mode Y as a function of the reduced magnetic field strength h. Curve 1: $\Phi = 1$ rad, $k_t = 0.1$, $k_b = 1.5$; curve 2: $\Phi = 0.6$ rad, $k_t = 0.1$, $k_b = 1.5$; curve 3: $\Phi = 1$ rad, $k_t = 0.2$, $k_b = 1.5$; curve 4: $\Phi = 1$ rad, $k_t = 0.1$, $k_b = 0.8$.

Figure 11 shows the ranges of occurrence of the three states in the plane (Φ, h) for chosen sets of material parameters. The range Δh of the magnetic field strengths, which induce the stripes, decreases with the twist angle Φ. There exists a critical maximum twist angle Φ_Y at which Δh shrinks to a point $h_D = h_P = 1$. The spatial period diverges to infinity when Φ tends to Φ_Y at constant field $h = 1$ (figure 5). Above Φ_Y, the only possible states are HD and US. The critical twist angle Φ_Y and Δh decrease with k_t and k_b. The biggest ranges of Φ and k_t, for which the Mode Y exists, arise for $h = 1$. The corresponding range of occurrence of Y-type stripes in the plane (Φ, k_t) is presented in figure 6 (below the curve 2). The ranges of occurrence of the stripes in the (k_t, h) plane, possess wedge-like shapes similar to those existing in the (Φ, h) plane presented in figure 11.

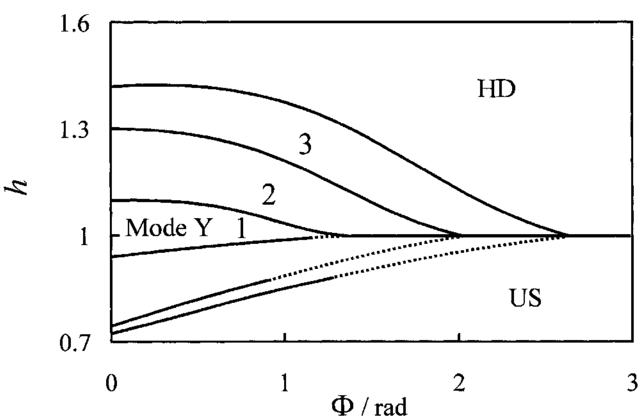

Figure 11. The ranges of existence of Mode Y in the (Φ, h) plane. Region 1: $k_t = 0.2$, $k_b = 1.5$; region 2: $k_t = 0.1$, $k_b = 1.5$; region 3: $k_t = 0.1$, $k_b = 0.8$. Dotted parts of the lower boundaries denote the hysteretic behaviour.

In the case of homogeneous deformations of the twisted chiral nematic layers, the transitions between the US and HD states can be of first or second order. In the former case, the deformation arises discontinuously at the threshold field H_{TN} and also decays discontinuously at a slightly lower field. These rapid changes have found application in super-twisted nematic displays. The condition for this hysteretic behaviour can be given in the form of the inequality [3, 16]

$$\frac{\Phi}{\pi} > \{(s-2)\tau + [\tau^2(s-2)^2 + (s^2 - s + 1)(s - \tau^2)]^{1/2}\} / (s^2 - s + 1) \qquad (2)$$

where $\tau = 2d/p$ and $s = k_b/k_t$. In particular, the hysteresis occurs for sufficiently high Φ and low k_t. At $h = 1$, finite deformation characterized by non-zero amplitudes θ_m and φ'_m can be observed. The consequences of this behaviour can be seen in our results obtained for Mode Y. They are illustrated by the amplitudes θ_m of the periodic deformations plotted versus the twist angle, figure 12(*a*), and versus the reduced magnetic field, figure 12(*b*). In figure 12(*a*), three examples of the $\theta(\Phi)$ dependence calculated for $h=1$ are shown. Two types of behaviour may be noticed. For high k_t, the amplitudes decay continuously with Φ and became zero for $\Phi = \Phi_Y$. This corresponds to the fact that for $\Phi > \Phi_Y$, the homogeneous deformation of the layer at $h = 1$ does not yet arise, since criterion (2) is not satisfied. In the opposite case, when k_t is sufficiently low, the amplitudes remain finite for $\Phi = \Phi_Y$. This is consistent with the significant homogeneous deformation which takes place at $h = 1$ for $\Phi > \Phi_Y$, since the condition for hysteresis is fulfilled.

Another manifestation of this effect is shown by the $\theta(h)$ plots, figure 12(*b*). When k_t is sufficiently low and Φ is sufficiently high, the finite amplitude reveals the occurrence of hysteresis (curve 1). In the opposite cases, for too high a value of k_t (curve 2) or too low a value of Φ (curve 3), the periodic deformations arise continuously, i.e. $\theta_m = 0$ at $h = h_P$. These examples suggest that a criterion analogous to inequality (2) could be formulated for the transition US–PD.

3.3. *Coexistence of Modes X and Y*

For some ranges of parameters, both modes may potentially exist in the same sample as shown in figures 13 and 6. The mode with the lower free energy should be realized in practice. The approximate boundary between two coexisting modes, based on this criterion, is plotted in figures 13 and 6 as a dashed line. Mode Y is preferred on the left of the boundary, whereas Mode X is favoured on the right of it.

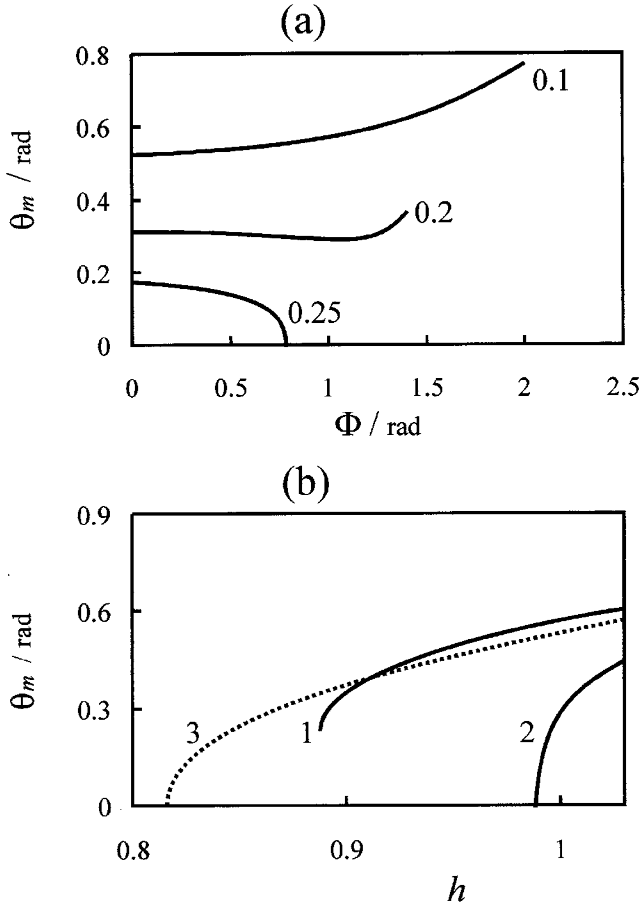

Figure 12. The hysteretic behaviour of Mode Y illustrated by the amplitudes θ_m plotted as functions of the twist angle Φ (*a*) and of the reduced magnetic field strength h (*b*). $k_b = 1.5$; (*a*) $h = 1$, k_t values are indicated on each curve; (*b*) curve 1: $\Phi = 1$ rad, $k_t = 0.1$; curve 2: $\Phi = 1$ rad, $k_t = 0.2$; curve 3: $\Phi = 0.6$ rad, $k_t = 0.1$.

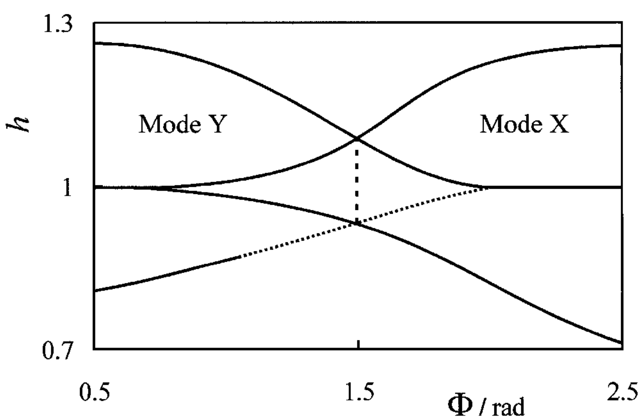

Figure 13. Overlapping of the ranges of existence of the two modes; $k_t = 0.1$, $k_b = 1.5$; dashed line is the boundary between them, corresponding to equality of energies; dotted part of the curve denotes the hysteretic behaviour of Mode Y.

3.4. *Influence of surface tilt*

It is known that deviation from ideal planar alignment quenches the periodic deformations [7, 8]. To study this effect we adopted small non-zero surface tilt angles δ and considered the Mode X in super-twisted nematic material with typical elastic properties ($k_b = 1.5$, $k_t = 0.6$; $\Phi = \pi$). In the case of non-zero δ, one sense of the deformation, i.e. one sign of the angle θ, is preferred. For this reason one of the two parts of the stripe is wider than the other. This effect is illustrated in figure 14, where the profiles of the angles $\theta(\xi, 0)$ and $\varphi'(\xi, 0)$ are plotted. The resulting asymmetry is measured by the parameter w equal to the ratio of the widths of both parts of the stripe. As the asymmetry increases with δ, w decreases as shown in figure 15. Simultaneously the stripe widens, which is also presented in figure 15 by the plot of the $Q(\delta)$ function. Only one nearly homogeneous region develops in the preferred part of the stripe. For some critical surface tilt, determined by $Q = 0$ and $w = 0$, it spreads over the whole layer, which means that the periodic deformation is replaced by one that is homogeneous.

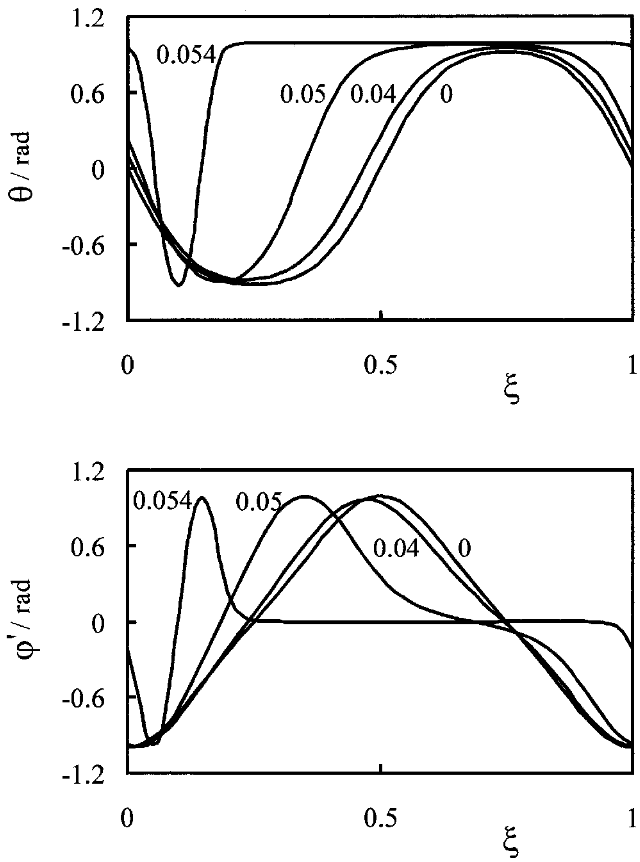

Figure 14. The profiles of the angles θ and φ' in the case of non-zero surface tilt for $\zeta = 0$. $\Phi = \pi$, $k_t = 0.6$, $k_b = 1.5$, $h = 1$; the tilt angles δ (in radians) are indicated for each curve.

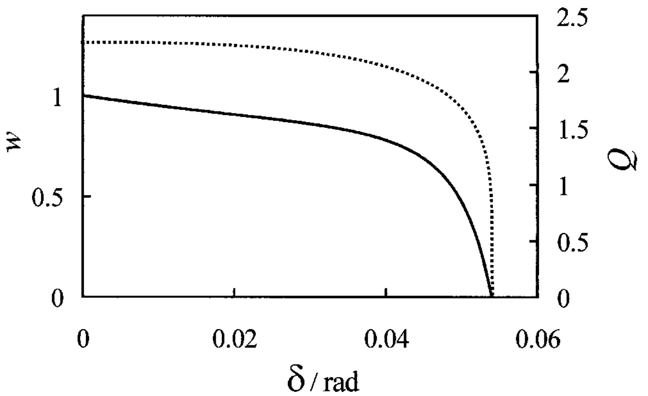

Figure 15. The asymmetry parameter w (full line) and the dimensionless wave number Q (dotted line) of Mode X as a function of the tilt angle δ. $\Phi = \pi$, $k_t = 0.6$, $k_b = 1.5$, $h = 1$.

3.5. *Non-chiral nematics*

Non-chiral nematics cannot be twisted by angles greater than $\pi/2$. Our calculations for this class of material show that Mode Y occurs in the same range of parameters as in the case of chiral nematics, i.e. conditions of sufficiently low k_t and Φ. The $Q(h)$ and $Q(\Phi)$ relations coincide with those presented in figures 5 and 10. The differences are so small that no corresponding curves were drawn in the figures.

We restricted our considerations of Mode X to $\Phi = \pi/2$ which is used in twisted nematic displays. We found that for given material constants, they are much wider than the Y stripes, which was also reported in [4]. The stripes occurred only for low k_t. Sufficiently high k_b values were necessary to assure stripe stability. For typical k_b, Mode X was energetically unfavourable with respect to Mode Y. As the stripes arise in a typical chiral nematic, one can conclude that the chirality favours their occurrence. The above results indicate that TN cells filled with typical nematic materials do not suffer periodic deformations.

4. Discussion

In this paper, the results of numerical calculations concerning the stationary periodic deformations induced by a magnetic field in planar twisted-nematic layers are presented. The main achievements of our work are as follows:

(i) Two types of stripe, called Mode X and Mode Y, with wave vectors parallel and perpendicular to the initial mid-plane director, respectively, were recognized. It should be emphasized that the directions of the wave vectors of both modes, the symmetry of the $\theta(\zeta)$ and $\varphi'(\zeta)$ functions and the phase shift between the $\theta(\xi)$ and $\varphi'(\xi)$ (or $\theta(\eta)$ and $\varphi'(\eta)$) dependences have been obtained as an effect of minimization of the free energy on the preliminary stage of the computations. With one exception mentioned in (ii) below, they are consistent with properties of the periodic modes considered by Kini [4, 5].

The X stripes with $\mathbf{q} \parallel \mathbf{n}_0(\zeta = 0)$ obtained for typical material parameters correspond to the stripes observed by Chigrinov *et al.* [2]. A qualitative comparison with some of their experimental data is possible. The reduced threshold voltage, defined in analogy to h_P as $u_P = U_P/U_{TN}$ (where U_{TN} is the threshold voltage for the homogeneous deformation), decreased with the twist angle. The width of the stripes also decreased with Φ. These statements agree with our relations $Q(\Phi)$ and $h_P(\Phi)$ (figures 4 and 5, respectively). Our values of Φ_X are also consistent with the reported data.

(ii) The equilibrium director distributions within single stripes of both modes were revealed. The nature of the difference between the structures of Modes X and Y is most evident for strong deformations. In a simplified way, both structures can be described as a result of the following process. Let us consider a layer as defined in § 2. The layer can be deformed homogeneously with positive or negative values of θ. Let the layers with both senses of deformation be divided by the planes perpendicular to the x axis into slabs of width $\lambda/2$. Two slabs, taken from different layers and put together, form an approximate model of a single stripe of Mode X. Mode Y arises in an analogous way when the dividing planes are normal to the y axis. This procedure reflects the important feature of the stripes, namely the origin of the homogeneous regions which are involved in the transition from the PD to HD states.

The evolution of the symmetry properties of Mode X was stated. The functions $\theta(\zeta)$ and $\varphi'(\zeta)$ are both even in a weakly deformed layer (in agreement with [4] and [5]) which is not in conformity with the properties of the HD state. In an increasing field, the character of these functions varies and they are neither odd nor even. Further increase in the magnetic field strength leads to formation of homogeneously deformed regions which possess the symmetry properties of the HD state (i.e. $\theta(\zeta)$ is even and $\varphi'(\zeta)$ is odd).

The analogy between the structures of Mode Y and the PST stripes was found. It is manifested by the symmetry of the $\theta(\zeta)$ and $\varphi'(\zeta)$ functions which is identical for both types of deformation. Mode Y can be considered as a twisted variant of the PST deformation observed for $\Phi = 0$.

(iii) The character of the transition from the PD to HD states is recognized as a result of infinite divergence of the stripe width. The drastic deviation of functions $\theta(\xi)$ and $\varphi'(\xi)$ (or $\theta(\eta)$ and $\varphi'(\eta)$) from sinusoidal form is observed at high field. The nearly homogeneous regions arise in each half of a stripe. The divergence of the spatial period with the field strength is accompanied by spreading of the homogeneous regions over the whole layer which is equivalent to a PD $\rightarrow$ HD transition. This suggests a continuous character for this transition in contrast to the discontinuous behaviour for cholesteric layers which was predicted from the criterion of equal energies of both types of deformation [8–11]. A similar mechanism of transition from a periodically deformed to a homogeneously deformed state has also been found in other systems [12, 13].

(iv) The hysteresis at the onset of Mode Y was found for particular parameters of the layer. The transition PD $\rightarrow$ US was usually accompanied by decay of the amplitudes θ_m and φ'_m to 0. However, for low k_t or sufficiently high Φ, the amplitudes of Mode Y remained finite at the critical field h_P and in a narrow interval δh below h_P, which reflects the presence of hysteresis at the deformation onset. The boundaries $h(\Phi)$ between the US and Mode Y regions, shown in figures 11 and 13, are based on the $\theta_m(h)$ dependences calculated for various Φ and were determined as the field strength at which θ_m reached zero. For the continuous transition, this procedure yielded the threshold h_P. For a discontinuous transition, the result was smaller than h_P by the width of the hysteresis δh. Nevertheless, we have plotted approximately the corresponding parts of the $h_P(\Phi)$ curves in figures 11 and 13 as dotted lines, since the biggest δh is about 0.05 and we neglected it.

(v) The quenching of the PD state by the surface tilt reported earlier [7, 8] was confirmed. The influence of the surface tilt on the X stripe structure was determined. The decay of Mode X caused by the surface tilt was explained as a consequence of development of one preferred sense of deformation consistent with the surface tilt.

(vi) The essential role of chirality for the occurrence of Mode X in typical nematic materials was established for $\Phi < \pi/2$. On the other hand, the effect of chirality on Mode Y was found to be negligible. The calculations for chiral nematics were performed under the assumption that the pitch was compatible with the twist angle in order to assure analogous circumstances of deformation for various twist angles. Our results suggest that for other relations between Φ and p, the qualitative features of the periodic deformations would be the same, although different ranges of existence of the stripes should be expected.

(vii) The ranges of parameters which favour the periodic patterns were determined. Sufficiently high twist angle Φ favours Mode X and sufficiently small Φ and k_t are necessary for Mode Y which agrees qualitatively with earlier results [4, 5, 8–11]. Therefore, Mode X can be observed in typical low molecular mass nematics, whereas Mode Y should be sought in polymeric or lyotropic materials with high elastic anisotropy like PBG [2, 17]. When both modes may coexist, two equivalent criteria for their realization can be adopted: the mode with the lower critical field [4, 5] or with the lower energy is preferred.

References

[1] Chigrinov, V. G., Belyaev, V. V., Belyaev, S. V., and Grebenkin, M. F., 1979, *Zhurnal exp. teor. Fiz.*, **77,** 2081 [1979, *Sov. Phys. JETP*., **50,** 994].
[2] Lonberg, F., and Meyer, R., 1985, *Phys. Rev. Lett*., **55,** 718.
[3] Raynes, E. P., 1986, *Mol. Cryst. liq. Cryst. Lett*., **4,** 1.
[4] Kini, U. D., 1987, *J. Phys*., **48,** 1187.
[5] Kini, U. D., 1987, *Mol. Cryst. liq. Cryst*., **153,** 1.
[6] Scheffer, T., and Nehring, J., 1997, *Annu. Rev. mater. Sci*., **27,** 555.
[7] Tsoy, V. I., Simonenko, G. V., and Chigrinov, V. G., 1993, *Liq. Cryst*., **13,** 227.
[8] Schiller, P., and Schiller, K., 1990, *Liq. Cryst*., **8,** 553.
[9] Schiller, P., 1990, *Phase Trans*., **29,** 59.
[10] Schiller, P., 1990, *Mol. Cryst. liq. Cryst*., **180B,** 177.
[11] Schiller, P., 1989, *Liq. Cryst*., **6,** 383.
[12] Krzyżański, D., and Derfel, G., 2000, *Phys. Rev. E*, **61,** 6663.
[13] Krzyżański, D., and Derfel, G., 2001, *Phys. Rev. E*, **63,** 021702.
[14] Oldano, C., 1986, *Phys. Rev. Lett*., **56,** 1098.
[15] Zimmermann, W., and Kramer, L., 1986, *Phys. Rev. Lett*., **56,** 2655.
[16] Derfel, G., 1988, *Liq. Cryst*., **3,** 1411.
[17] Taratuta, V. G. Hurd, A. J., and Meyer, R. B., 1985, *Phys. Rev. Lett*., **55,** 246.